Molecular Crystals and Liquid Crystals Incorporating Nonlinear Optics

Publication details, including instructions for authors and subscription information:
http://www.tandfonline.com/loi/gmcl17

Rheological Properties of Nematic Solutions of Rodlike Polymers

G. C. Berry [a]

[a] Department of Chemistry, Carnegie-Mellon University, Pittsburgh, Pennsylvania, 15213

Version of record first published: 03 Jan 2007.

To cite this article: G. C. Berry (1988): Rheological Properties of Nematic Solutions of Rodlike Polymers, Molecular Crystals and Liquid Crystals Incorporating Nonlinear Optics, 165:1, 333-360

To link to this article: http://dx.doi.org/10.1080/00268948808082206

Mol. Cryst. Liq. Cryst., 1988, Vol. 165, pp. 333–360
Reprints available directly from the publisher
Photocopying permitted by license only

Printed in the United States of America

Rheological Properties of Nematic Solutions of Rodlike Polymers

G. C. BERRY

Department of Chemistry, Carnegie-Mellon University, Pittsburgh, Pennsylvania 15213

(*Received December 23, 1987*)

The rheological properties of nematic solutions of rodlike polymers are discussed. Comparisons are made with the behavior of isotropic solution of rodlike polymers as well as that of small molecule nematogens. Evaluation of the Frank elastic constants and the Leslie-Ericksen viscosity coefficients by light scattering methods is discussed, along with theoretical prediction of the latter of rodlike systems. The nature of shear deformation over a wide range of shear rates is discussed in terms of possible flow instabilities revealed by rheological and rheo-optical observations.

1. INTRODUCTION

It has long been known that solutions of nematogenic polymers exhibit peculiar flow behavior with increasing concentration c of the polymer as c is increased beyond the value c_{NI} required to form a nematic phase.[1] For example, although a limiting viscosity η_0 is found under steady-state shear at small shear rate for $c < c_{NI}$, for $c > c_{NI}$ the apparent viscosity seems to increase without limit as the deformation rate is reduced, being essentially a constant η_p over a range of rates that are neither too slow nor too fast.[2-8] Whereas η_0 increases with $c < c_{NI}$, η_p decreases with increasing c somewhat in excess of c_{NI}, see below.[1-7] The linear and nonlinear viscoelastic behavior of isotropic solutions of rodlike nematogenic polymers ($c < c_{NI}$) is reasonably well characterized by experiment and understood theoretically.[8,9] For a usefully wide range of deformation rates the behavior can be fitted by a single-integral constitutive equation, see below. By contrast, the viscoelastic behavior of nematic solutions of rodlike

polymers with $c > c_{NI}$ is neither completely characterized experimentally nor treated theoretically.

The situation with nematogenic polymers stands in contrast to studies on the flow behavior of small molecule nematogens. With the latter, viscoelastic behavior is absent, and rheological behavior is understood in terms of the "Leslie-Ericksen" constitutive equation for the (viscous) stress tensor $\sigma^{(v)}$, which gives[9-12]

$$\sigma^{(v)} = \alpha_1(\boldsymbol{nn}:\boldsymbol{A})\boldsymbol{nn} + \alpha_2\boldsymbol{nN} + \alpha_3\boldsymbol{Nn} + \alpha_4\boldsymbol{A} + \alpha_5\boldsymbol{nn}\cdot\boldsymbol{A} + \alpha_6\boldsymbol{A}\cdot\boldsymbol{nn} \quad (1a)$$

where the α_i are material constants (it is usually assumed that $\alpha_6 = \alpha_2 + \alpha_3 + \alpha_5$),[13] $\boldsymbol{n}$ is the unit vector called the director, oriented along the axis of uniaxial symmetry of the nematic phase, and

$$\boldsymbol{n} \times (\boldsymbol{h} - (\alpha_3 - \alpha_2)\boldsymbol{N} - (\alpha_2 + \alpha_3)\boldsymbol{A}\cdot\boldsymbol{n}) = 0 \quad (1b)$$

$$\boldsymbol{A} = \frac{1}{2}(\boldsymbol{\kappa} + \boldsymbol{\kappa}^{+}) \quad (1c)$$

$$\boldsymbol{N} = \frac{d\boldsymbol{n}}{dt} - \frac{1}{2}(\boldsymbol{\kappa} - \boldsymbol{\kappa}^{-})\cdot\boldsymbol{n} \quad (1d)$$

with $\boldsymbol{\kappa}$ the velocity gradient tensor and $\boldsymbol{n} \times \boldsymbol{h}$ the torque per unit volume resulting from an external field or spatial inhomogeneity of the director. The latter are analyzed through an elastic free energy density W expressed as[10,12]

$$2W = K_S(\text{div } \boldsymbol{n})^2 + K_T(\boldsymbol{n}\cdot\text{curl } \boldsymbol{n})^2 + K_B(\boldsymbol{n}\times\text{curl } \boldsymbol{n})^2 \quad (2)$$

where the Frank elastic constants K_S, K_T and K_B for splay, twist and bend distortions, respectively, are material dependent. A number of flow situations have been analyzed with these relations, including stable flow in the presence or absence of an external field, and flow instabilities that develop under a variety of conditions.[10-12,14-16]

In the following we will discuss the rheological behavior of nematic solutions of rodlike polymers, both in comparison with counterpart isotropic solutions with $c < c_{NI}$, and where appropriate with the behavior of small molecule nematogens.

2. RHEOLOGICAL BEHAVIOR OF ISOTROPIC SOLUTIONS OF RODLIKE POLYMERS

For the deformation rates of interest in this study the single-integral equation

$$\sigma_M(t) = \Sigma\eta_i\tau_i^{-2}\int_0^\infty [\Delta\gamma(t, u)]^M F(\Delta\gamma(t, u))\exp(-u/\tau_i)du \quad (3)$$

provides a satisfactory representation of the shear stress $\sigma(t) = \sigma_1(t)$ and the first normal stress difference $\nu^{(1)}(t) = \sigma_2(t)$ for isotropic solutions of rodlike polymers.[8] Here, $\Delta\gamma(t, u) = \gamma(t) - \gamma(t - u)$, with $\gamma(s)$ the strain at time s, $F(\Delta\gamma)$ a function known with reasonable accuracy,[8,9] and η_i and τ_i constants appearing in the expression for the (linear) shear modulus $G(t)$:

$$G(t) = \Sigma\,\eta_i\tau_i^{-1}\exp(-t/\tau_i) \quad (4)$$

where the η_i are so normalized that $\eta_0 = \Sigma\,\eta_i$. Moreover, the birefringence $\Delta n_{13}(t)$ observed for light propagated perpendicular to the flow plane for flow between parallel plates may be expressed as

$$\Delta n_{13}(t) = C'\,\nu^{(1)}(t) \quad (5)$$

where C' is a stress-optic constant.[8,17]

A theoretical treatment[9] leading to a result similar to Eq. (3) for a certain distribution of relaxation times and a specific $F(\Delta\gamma)$ expresses the stress tensor $\sigma_{\alpha\beta}(t)$ as a function of the (traceless) orientation tensor $S_{\alpha\beta}$, where

$$S_{\alpha\beta} = \langle \boldsymbol{u}_\alpha \boldsymbol{u}_\beta \rangle - \delta_{\alpha\beta}/3 \quad (6)$$

with $\mathbf{u}$ a unit vector along the axis of the rodlike chain and the brackets indicating an ensemble average. Both linear and nonlinear behavior are computed from the effects of flow on $S_{\alpha\beta}$, which is zero for the isotropic fluid at equilibrium. The nonlinear behavior represented in Eq. (3) reflects a decreasing tendency for orientation with increasing deformation rate, as compared with the rate of change of $S_{\alpha\beta}$ in the linear behavior in slow flow.

The material specific parameters η_i and τ_i may be determined by measurement of $G(t)$ or equivalently, may be computed from meas-

urements of the linear recoverable compliance $R_0(t)$ and the viscosity η_0 through use of the relation[18]

$$\int_0^t [R_0(u) + u\eta_0^{-1}]G(t - u)du = t \tag{7}$$

Use of η_i and τ_i so obtained and an expression for $F(\Delta\gamma)$ then permits calculation of $\sigma(t)$ and $\Delta n_{13}(t)$ for a variety of strain histories. Examples of experimental and calculated steady-state behavior obtained at shear rate κ for the viscosity $\eta_\kappa = \sigma/\kappa$ in the reduced form η_κ/η_0 and the birefringence in the reduced form $\Delta n_{13}/R_0(\kappa\eta_k)^2$ are given in Figure 1. The reduced shear rate $\tau_C\kappa$ is used in Figure 1, where $\tau_C = R_0\eta_0\kappa$, with $R_0 = R_0(\infty)$ the linear recoverable compliance; τ_C represents an weighted average over the τ_i.[18] The data shown in Figure 1 where obtained with isotropic solutions of the rodlike polymer[8]

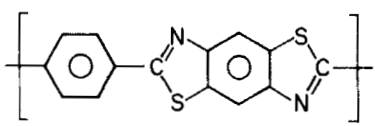

PBT

Similar behavior is observed with other rodlike chains or helicodal chains, e.g., the rodlike chains[2,5,6,19]

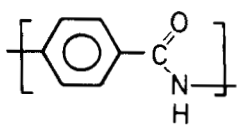

PBA

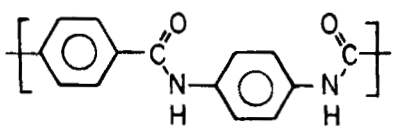

PPTA

or the helicodal chain[3,20]

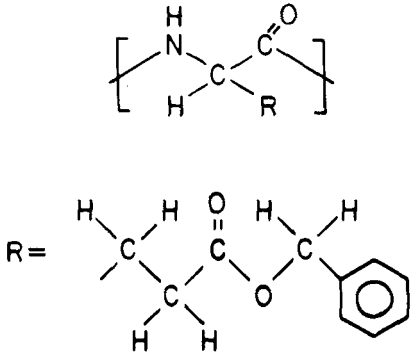

PBG

The theoretical estimate for $G(t)$ is essentially given by Eq. (4) with one term, with $\tau_1 = \tau_C$.[9] By contrast, experimental $G(t)$ require the use of several terms, with τ_i spanning several decades.[8] The theoretical treatment gives

$$\eta_0 = \eta_S K N_A{}^2 M[\eta](cL/M_L)^3(1 - Bc/c_{NI})^{-2} \tag{8}$$

where c is the polymer concentration (wt/vol), L is the contour length of a rod with molecular weight M and intrinsic viscosity $[\eta]$, $M_L = M/L$, η_s is the solvent viscosity, and B and K are constants. The experimental data shown in Figure 2 have been fitted by Eq. (8) with $B \approx 1$ and K of order 10^{-4}.[8] The estimate for B is similar to theoretical expectations, but the experimental K is much smaller than the original theoretical estimate.[9] The latter discrepancy is attributed to an erroneously large theoretical estimate of the disengagement time required for a rod to undergo an angular reorientation.[21,22]

3. TEXTURE AND MONODOMAIN FORMATION IN NEMATIC SOLUTIONS OF RODLIKE POLYMERS

The term texture refers to the global nature of the director field $\boldsymbol{n}$. As discussed in the following the observed texture is often far from equilibrium. For typical solutions of PBT and PPTA, the isotropic and nematic phases coexist for a narrow range of concentration for $c > c_{NI}$, with the istropic phase disappearing at roughly $1.1\ c_{NI}$.[8,19]

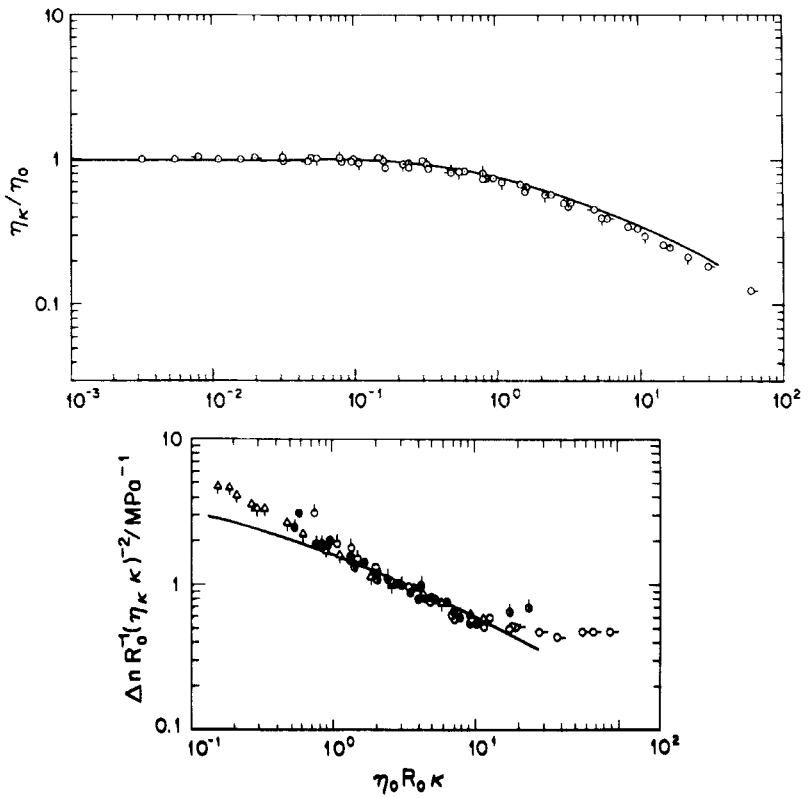

FIGURE 1 The viscosity η_κ (upper) and flow birefringence Δn (lower) for as a function of the shear rate κ for isotropic solution of the rodlike polymer PBT; η_0 and R_0 are the limiting values of the viscosity and the recoverable compliance, respectively, for small κ. The symbols designate different temperatures as discussed in Reference 8, and the curves are computed with Eq. (3) as discussed in the same reference (After Reference 8).

Since c_{NI} increases with increasing temperature for the specified systems; it is possible to quench a solution between two plates from a temperature for which $c < c_{NI}$ to a temperature for which the same concentration, $c > 1.1\ c_{NI}$, resulting in a nematic phase. In such a case a mottled texture develops initially, owing to the variation of $\boldsymbol{n}$ with position. This texture is sometimes described as a domain structure, implying the existence of regions in which $\boldsymbol{n}$ is nearly uniform, with $\boldsymbol{n}$ different in adjacent regions.[23] Any such regions might be separated by less ordered (perhaps isotropic) boundary layers. A mottled texture scatters light strongly, and when viewed with white light between crossed polars, it exhibits multicolored regions of vary-

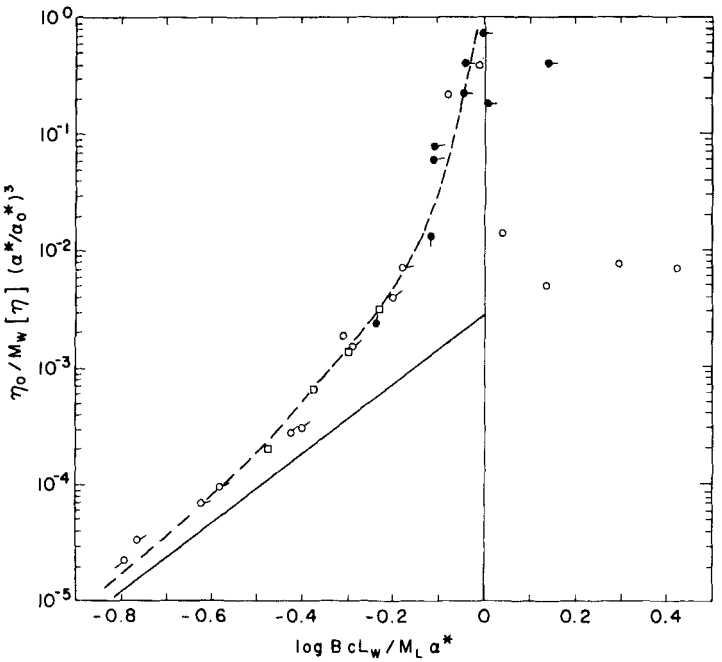

FIGURE 2 The dependence of the viscosity on concentration and chain length for solutions of the rodlike polymer PBT and PPTA; the viscosity is η_0 or η_p (as discussed in the text) for $BcL_W/M_L\alpha^*$ less than unity (isotropic solutions) or greater than unity (nematic solutions, respectively, $\alpha^* = C_{NI}L_W/M_L$ and B and α_0^* are constants. The curve is computed according to Eq. (8). The symbols designate different polymers as discussed in Reference 7. (From Reference 7).

ing transmission. Both of these features are consistent with a domain structure, but could also reflect extensive, but more-or-less continuous spatial variation of $\boldsymbol{n}$ throughout the fluid. Such a texture is not at equilibrium, but transforms slowly to a smooth equilibrium texture, characterized by much suppressed light scattering, and slow to negligible spatial variations of $\boldsymbol{n}$. The latter may be fixed by the orientation of adsorbed chains at confining surfaces, see below.

In general, the nematic phase may be characterized by the order parameter S given by[9,12]

$$S = (3\ \langle(\boldsymbol{u} \cdot \boldsymbol{n})^2\rangle - 1)/2 \tag{9}$$

such that at equilibrium, the orientation tensor becomes

$$S_{\alpha\beta} = S(n_\alpha n_\beta - \delta_{\alpha\beta}/3) \tag{10}$$

where $\boldsymbol{u}$ is a unit vector along the rodlike axis, and the angular brackets indicate an ensemble average; S is expected to be independent of position.[9,12] Under appropriate conditions, the transmission T_β for polarized light propagated through a sample, measured with an analyzer set at angle β to the polarizer, may be used to determine S, through the dependence of T_β on the retardation δ[24]:

$$T_\beta = K_\gamma[\cos^2\beta - \sin^2(\delta/2)\sin[2(\gamma - \beta)]\sin 2\gamma] \tag{11}$$

where γ is angle between the polarizer and the direction of maximum refractive index in the plane perpendicular to the light beam, the retardation is given by

$$\delta = 2\pi d\Delta n/\lambda \tag{12}$$

with Δn the birefringence for light with wavelength λ for a sample with thickness d, and $K_\gamma \leq 1$ accounts for attenuation due to scattering or absorption, the latter being dependent on γ if the sample is dichroic. Thus, T_+ calculated with $\beta = \pm\pi/2$ is given by (in the absence of absorption or scattering)

$$T_+ = \frac{1}{2}\sin^2(\delta/2)(1 - \cos 4\gamma) \tag{13}$$

Data shown in Figure 1 were obtained by the use of Eq. 13. Of course, the transmssion $T_\parallel$ with $\beta = 0$ or π is given by $1 - T_+$. In a nematic fluid with a uniaxial alignment measurement of T_+ and $T_\parallel$ under conditions with $\gamma = \pi/4$ and $\boldsymbol{n}$ in the plane perpendicular to the light beam permits evaluation of δ (mod π). Consequently, if the absolute value of δ is determined, then S may be computed given the refractive indices $n_\parallel$ and $n_\perp$ along and perpendicular to the rodlike axis, since $\Delta n = (n_\parallel - n_\perp)S$. Variations of $\boldsymbol{n}$ with position vitiates determination of S from measurements of T_+ and $T_\parallel$. For example, with the mottled texture, T_+ and $T_\parallel$, are about equal and do not vary with rotation of the sample between the polars if the sample is reasonably thick (e.g., > 100 μm). A similar texture develops if the nematic solution is rapidly agitated.

Because of the long equilibrium times to form a smooth texture, the majority of rheological measurements on nematic solutions of rodlike chains have been made on samples with a mottled texture. However, if allowed to stand for an extended period (typically 50 hr. or more), the mottled texture is replaced by a mostly smooth texture,

with a field of disclinations near either bounding surface.[25] The light scattering from the smooth texture is orders of magnitude less than that from the mottled texture; T_+ and $T_\parallel$ are not in general equal, and vary from place on the sample, and with rotation of the sample between the polars. A monodomain with uniform alignment of $\boldsymbol{n}$ may be created with nematic solutions of PBT by careful extrusion of the solution between the plates so that the molecules present at the advancing front are strongly oriented in an extensional flow.[25] These oriented chains are then adsorbed with preferential alignment in the flow direction. Consequently, on cessation of flow the fluoresence emitted by light absorbed close to the surface (e.g., a transmission length A/μ of about 300 nm for an absorbance A of 0.5, with μ the absorption coefficient) is strongly anisotropic even when sampled over a large surface area. By contrast, for samples prepared in the absence of an orienting flow the fluorescence is anisotropic only over a small surface area (e.g., $\sim 10^{-6}\text{cm}^2$), and is essentially isotropic over macroscopic dimensions. Although the sample is turbid immediately after cessation of flow (see below), an essentially defect free monodomain aligned in the flow direction results after a long annealing time (e.g, ca. 50 hr). For such a sample both T_+ and $T_\parallel$ depend markedly on the angle ψ between the polarizer and the flow direction. Thus T_+ is zero for $\psi = 0$ or 90 deg., and maximum for $\psi = 45$ deg. In addition, the sample is dichroic, textureless, and does not scatter light strongly. Similar monodomain samples have been reported for nematic solutions of other rodlike polymers.[26] The monodomain alignment may be driven by the preferential alignment of the adsorbed layer and/or the global preferential alignment of $\boldsymbol{n}$ along the flow direction in flow, albeit with large fluctuations from that alignment induced by unstable flow, see below.

4. RHEOLOGICAL PROPERTIES OF NEMATIC SOLUTIONS OF RODLIKE POLYMERS

Light scattering

Elastic and quasi-elastic light scattering measurements on monodomain samples provide information on the α_i and the Frank elastic constants defined above. Thus, the scattering provides the ratios K_S/K_T, K_B/K_T, η_S/K_T, η_B/K_T and η_T/K_T, and under favorable conditions may also be analyzed to give an absolute value of K_T.[12,26,27,28]

Here, η_S, η_B and η_T may be expressed in terms of the α_i by the relations

$$\eta_T = \alpha_3 - \alpha_2 \tag{14}$$

$$\eta_S = \eta_T - (\eta_{cb} - \eta_T)^2/4\eta_b \tag{15}$$

$$\eta_B = \eta_T - (\eta_{cb} + \eta_T)^2/4(\eta_{cb} + \eta_b) \tag{16}$$

where $\eta_{cb} = \eta_c - \eta_b = -\alpha_2 - \alpha_3$, with η_c and η_b the Miesowicz viscosities[29] for shear flow with $\boldsymbol{n}$ parallel to the velocity gradient and the flow direction, respectively:

$$2\eta_c = \alpha_4 + \alpha_5 - \alpha_2 \tag{17}$$

$$2\eta_b = \alpha_4 + \alpha_3 + \alpha_6 \tag{18}$$

Evidently, $\eta_T > \eta_S > \eta_B$ since $\eta_{cb} > 0$.[10] Results obtained with nematic solutions of PBT and PBG are given in Table I.[25,26] Theoretical calculations of the α_i for rodlike chains give results of the form

$$\alpha_i = \eta_0^{\mathrm{ISO}}(1 - S^2)^2 A_i(S) \tag{19}$$

where S is the order parameter at equilibrium, η_0^{ISO} is calculated from Eq. (8) with $B = 0$, and the $A_i(S)$ are functions of S.[9,30,31] The results for the $A_i(S)$ obtained with two approximate treatments based on the Leslie-Ericksen constitutive equation are given in Table II.[30,31,32] These theories give S as a function of $X = c/c_{\mathrm{NI}}$:

$$4S = 1 + 3[1 - 8/(9X)]^{1/2}; \qquad \text{Ref. 30} \tag{20a}$$

$$S = 1 - a_2X^{-2} - a_4X^{-4} - a_6X^{-6}; \text{ Ref. 31} \tag{20b}$$

where numerical estimates of the a_i are available (e.g., $a_2 = 0.147$). With either treatment, the viscosities may be expressed in terms of η_0^{ISO} and S, e.g.,

$$\eta_T = 6\eta_0^{\mathrm{ISO}} H_T(S) \tag{21a}$$

The entries in Table II give

$$H_T(S) = 3S^2(1 - S^2)^2/(2 + S); \text{ Ref. 30} \tag{21b}$$

$$H_T(S) = 5S^2(1 - S^2)/(5S - 2); \text{ Ref. 31} \tag{21c}$$

TABLE I

Experimental Frank elastic constants and Leslie viscosity coefficients

Polymer	K_S/K_T	K_B/K_T	η_S/η_T	η_B/η_T	η_T/K_T (Pa·s-pN^{-1})
PBT[a]	15.8	7.3	0.86	0.14	191
PBG[b]	11.3	13.1	0.99	0.006	9.6

[a]0.041 weight fraction PBT ([η] = 1800 ml/g); K_T is estimated to be 2.4 pN.[25]
[b]0.13 weight fraction PBG; K_T = 0.36 pN.[26]

With one of these treatments,[30] η_S and η_B are both zero for all S. Values of η_S/η_T, η_B/η_T and α_1/η_T obtained with the other treatment,[31] given by the expressions

$$\eta_S/\eta_T = 1 - 35/(80S^2 + 108S - 21) \tag{22}$$

$$\eta_B/\eta_T = 1 + 35(4S - 1)^2/3(40S^4 - 76S^3 - 96S^2 + 20S + 7) \tag{23}$$

$$\alpha_1/\eta_T = -(5S - 2)(4S - 1)/9 \tag{24}$$

are shown in Figure 3. Although this treatment gives $\eta_S/\eta_T > \eta_B/\eta_T$, as observed for the PBT solution, the experimental data are not fitted by the theory for any single value of S.

TABLE II

Theoretical Leslie-Ericksen coefficients for rodlike polymers

Parameters[a]	Reference 30	Reference 31[b]
α_1/k	$-S^2$	$-rS^2$
α_2/k	$-S(1 + 2S)/(2 + S)$	$-(S/2)[3(r - 1) + 2(1 + 2S)]/[3(r - 1) + 2 + S] = -S(4S - 1)/(5S - 2)$
α_3/k	$-S(1 - S)/(2 + S)$	$-(S/2)[3(r - 1) + 2(1 - S)[3(r - 1) + 2 + S] = S(1 - S)/(5S - 2)$
α_4/k	$(1 - S)/3$	$(7 - 5S - 2rS^2)/35 = (1 - S)[1 - (2/35)(1 - S)(7 + 4S)]/3$
α_5/k	S	$S(5 + 2rS)/7 = S[1 - (2/21)(1 - S)(3 - 4S)]$
α_6/k	0	$-2S(1 - rS)/7 = 2S(1 - S)(3 + 4S)/21$
λS[c]	$1 - (1 - S)/3$	$r - (1 - S)/3 = -1 - 5(1 - S)/3$
r	—	$1 - 4(1 - S)/3$

[a]$k = k'\eta_0^{ISO}(1 - S^2)^2$; η_0^{ISO} given by Eq. 8 with B = 0 and k' is 6 or 10 in references 30 and 31, respectively. Since $\alpha_2 + \alpha_3 = \alpha_6 - \alpha_5$, only five of the α_i are independent.
[b]Based on asymptotic behavior for α_i given in reference 31 and approximate relations for λ and r.[32]
[c]$\lambda = \eta_{cb}/\eta_T$, see Eqs. 26, 28.
(From reference 32)

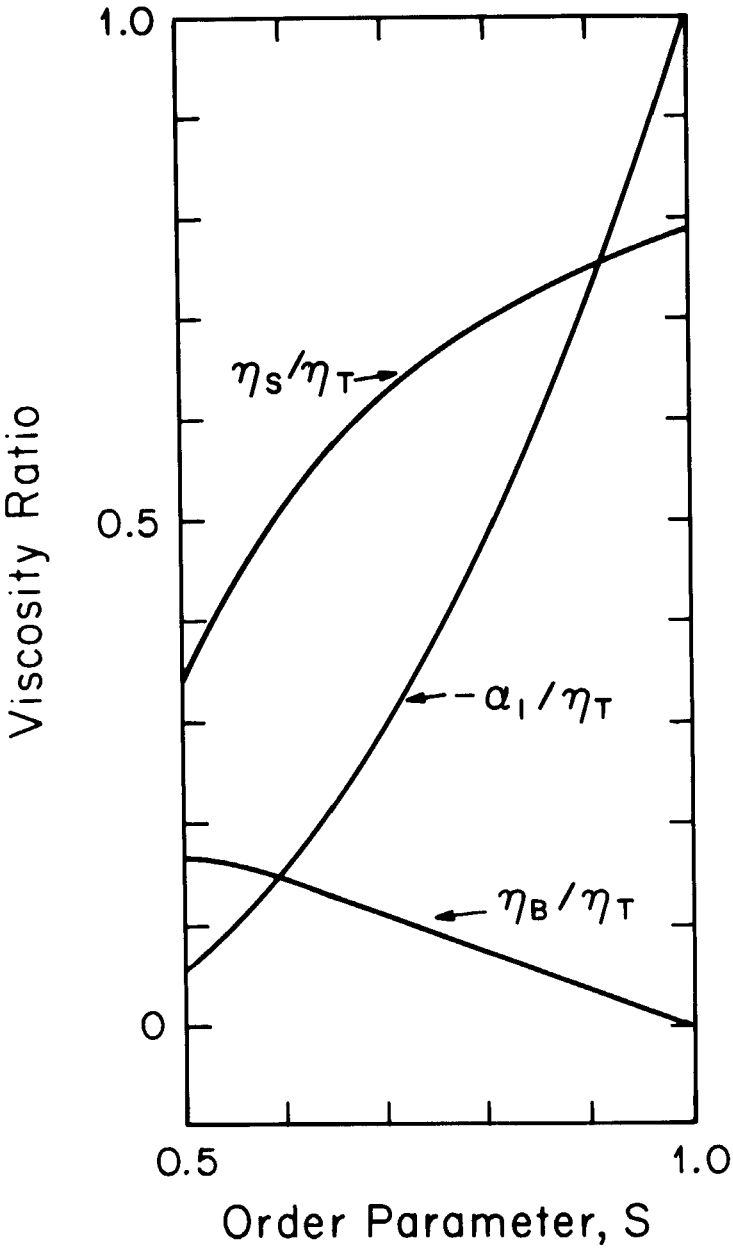

FIGURE 3 Vartious viscosity ratios as functions of the order parameter S, computed using Eqs. 22–24.

Flow induced by an external field

Distortion of the director alignment in an external field is frequently used to determine the Frank elastic constants with small molecule nematogens.[12] For example, a twist distortion might be created by application of a magnetic field H perpendicular to $\boldsymbol{n}$ and in the plane parallel to the boundary planes to which $\boldsymbol{n}$ is parallel. In this case, a distortion is expected if the field strength magnitude exceeds the critical value $H_C = (\pi/d)(K_T/|\Delta\chi|)^{1/2}$, where d is the separation between the plates and $\Delta\chi$ is the difference $\chi_\parallel - \chi_\perp$of the principle diamagnetic susceptibilities per unit volume, with $\chi_\parallel$ and $\chi_\perp$ the components along and perpendicular to $\boldsymbol{n}$, respectively.[12] The creation of the distortion may require flow, and with polymer solutions this may be slow enough to permit the visualization of intermediate director field alignments, providing information on the α_1. Analysis of such a flow is based on the use of Eq. 1a for the stress and the force balance

$$\partial_\beta p + \partial_\alpha \sigma_{\alpha\beta} = 0 \tag{25}$$

along with the balance of torques expressed by Eq. 1b, making use of Eq. (2) to express the torque per unit volume $\boldsymbol{n} \times \boldsymbol{h}$ resulting from the elastic distortions.[33] Bands parallel to $\boldsymbol{H}$ with alternating large and small transmission T_+ viewed with angle ψ between the polarizer and the analyzer of 45 deg. for solutions of PBG have a characteristic spacing L dependent on H/H_C, and are attributed to coupling between director rotation and shear flow.[33] A linearized analysis based on the assumption that the director remains everywhere parallel to the bounding surfaces gives a relation between H/H_C and L that depends on K_B/K_T, η_B/η_T, and η_c/η_a, where $\eta_a = \alpha_4/2$ is the viscosity with $\boldsymbol{n}$ perpendicular to both the flow direction and the velocity gradient.[33,34] In studies on aligned nematic solutions of PBT in the same geometry, the optical observations differ significantly:[35] when viewed with light polarized along the original director alignment (no analyzer), a series of alternating dark and bright bands aligned along $\boldsymbol{H}$ is found in focal planes l above and below the sample plane of symmetry, with the bright image the plane at l above the dark image in the plane at $-l$ and vice versa. No pattern is observed in intermediate focal planes, or with light polarized in the perpendicular direction. This optical effect is similar to that reported for an electric field applied perpendicular to the sample plane,[36] and in certain cases with a temperature gradient between the two bounding planes.[15] It is attributed to a circulatory flow in which the closed flow

lines are in the plane orthogonal to $\boldsymbol{H}$. The flow induces tilt of the director out of the original plane of symmetry, by an amount that is maximal in the center of a flow cell, where the tangential velocities are least, and minimal at the cell boundaries, where the velocities are largest.[36] The cells form cylinders with axes along $\boldsymbol{H}$. The separation L' of the bright images decreases with increasing H, and l^{-1} is linear in $(H/H_C)^2$ over the range studied. Although a theoretical analysis of this effect is unavailable, it can be expected to include the parameter K_S/K_T and η_S/η_T in the dependence of l on H.

Although apparently unexamined with polymeric nematogens, it should be possible to induce distortion of the director field and the associated coupled flow through interaction of light beam with the medium. Such effects observed in small molecule nematogens with laser beams of moderate intensity (ca. 10^2 watt/cm^2) have been analyzed with a suitable variation of Eq. 25.[37]

Behavior in slow flow

A typical flow curve is shown in Figure 4—the data shown are for a nematic solution of PBT,[7] but similar behavior is observed with PPTA, PBG and other nematic polymer solutions.[2,4–6,19] The parameter η_p used in Figure 4 is the viscosity in the "plateau region" for which the viscosity is about independent of the shear rate κ. Flow in this region is designated slow flow in the following. As seen in Figure 4, the recoverable compliance R_κ after steady flow at shear rate κ tends to a limiting value R_0, as with isotropic solutions, but η_κ increases above η_p with decreasing κ, and does not appear to reach a limiting value with decreasing κ. Flow in the region of small κ with $R_\kappa \approx R_0$, but η_κ increasing with decreasing κ is designated anomalous slow flow in the following. For $\eta_p R_0 \kappa > 1$, η_κ decreases below η_p with increasing κ, a region designated fast flow in the following. Anomalously slow flows and fast flows are discussed separately in subsequent sections.

Calculations with Eq. (1) in the absence of external fields ($h = 0$), including any effects of surface alignment, predict that shearing flow is stable provided $\alpha_2\alpha_3 > 0$, with a well defined uniform alignment of the director (constant $\boldsymbol{n}$) in the plane of shear at angle θ_0 to the flow direction.[10] In general, if shear flow is stable, η_0 may be expressed in the form (for $h = 0$)[10]

$$\eta_0 = \eta_b + (1/2)(1 - \lambda^{-1})[\eta_{cb} + \alpha_1(1 + \lambda^{-1})/2] \qquad (26)$$

where η_b and η_{cb} are defined above and $\lambda = \eta_{cb}/\eta_T > 1$ for stable

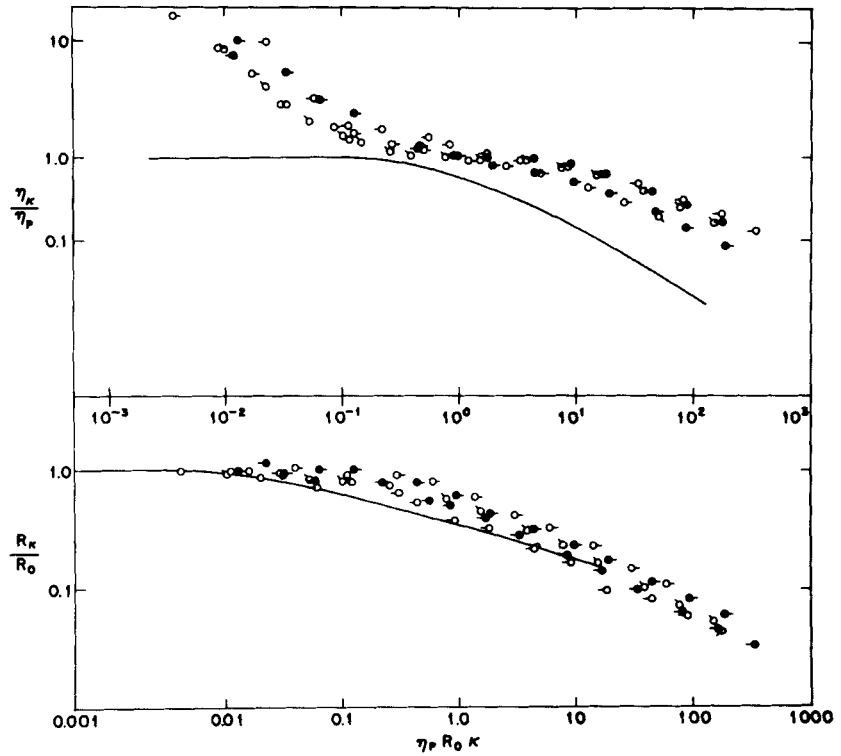

FIGURE 4 The viscosity η_κ and the recoverable compliance R_κ as functions of shear rate κ for nematic solutions of PBT; the symbols designate different temperatures and concentration as discussed in Reference 7. The quantity η_p is a "plateau viscosity" determined as discussed in the text. The solid curve show η_κ/η_0 and R_κ/R_0 versus $\eta_0 R_0 \kappa$ for isotropic solutions of the same PBT polymer. (From Reference 7).

flow, and $2\theta_0 = \arccos \lambda^{-1} = 2\arctan(\alpha_3/\alpha_2)^{1/2}$. As shown by Eq. 26, η_0 tends to η_b as θ_0 tends to zero. Making use of Eq. 19 for rodlike chains,

$$\eta_0 = \eta_0^{ISO} H_{Sh}(S) \tag{27}$$

where η_0^{ISO} is defined above (see Eq. 19) and $H_{Sh}(S)$ is a function of the equilibrium order parameter S, see below for discussion of $H_{Sh}(S)$. For our purposes it is convenient to express Eq. 26 in the form

$$\frac{\eta_0}{\eta_T} = \lambda[(\eta_S/\eta_B) - 1]^{-1} + \frac{1}{2}(\lambda - 1)[1 + (\alpha_1/\eta_T)(1 + \lambda)/4\lambda^2] \tag{28a}$$

where λ is given by

$$2\lambda = r + (r^2 - 4)^{1/2} \tag{28b}$$

$$r = 2\left[\frac{\eta_S}{\eta_T} - 2\frac{\eta_S}{\eta_T}\cdot\frac{\eta_B}{\eta_T} + \frac{\eta_B}{\eta_T}\right]\left[\frac{\eta_S}{\eta_T} - \frac{\eta_B}{\eta_T}\right]^{-1} \tag{28c}$$

With the data for the PBT solution given in Table I, $\theta_0 = 22$ deg., and $\eta_0/\eta_T = 0.46 + 0.06(\alpha_1/\eta_T)$, whereas for the PBG solution in Table I, $\theta_0 = 5$ deg.

Although comparison of Eq. 26 with observed viscosities is compromised by the analomous flow for very small κ (see below), it is universally found that η_p observed in slow flow is less than η_0 (extrapolated) for an isotropic solution of the same c and L,[1,2,4,5,8] as shown in Figure 2 for solutions of PBT.[8] If it is assumed that $\eta_p \approx \eta_0$ for the nematic solution, then for the PBT solution designated in Table I, $\eta_0/\eta_T \approx \eta_p/\eta_T = 0.21$, so that $\alpha_1/\eta_T < 0$, in qualitative accord with the behavior given in Figure 3. On the other hand, for the theory giving α_1 in Figure 3, $\eta_{cb} < \eta_T$, with the consequence that shear flow is predicted to be unstable. By contrast, for the theoretical treatment that gives $\eta_S = \eta_S = 0$,[30] $\eta_T < \eta_{cb}$, with η_0 given by Eq. 27 with

$$H_{Sh}(S) = \frac{(1 - S)^4(1 + S)^2(1 + 2S)(1 + 3S/2)}{(1 + S/2)^2} \tag{29}$$

Use of Eq. 20a for S in Eq. 29 gives η_0 as a decreasing function of increasing c, in qualitative accord with experiment shown in Figure 2.

The first normal stress difference $\nu^{(1)}$ has been computed on the basis of Eq. (1). For slow flow with $h = 0$ on materials $\alpha_2\alpha_3 > 0$, $\nu^{(1)}$ is predicted to be proportional to the shear stress, or

$$\nu^{(1)} = \eta_n|\kappa| \tag{30}$$

where η_n may be regarded as a normal viscosity.[9,31] By contrast, with isotropic fluids, $\nu^{(1)} \propto \kappa^2$ for small κ.[18,38] Making use of Eq. 19, η_n may be expressed in the form

$$\eta_n = \eta_0^{\mathrm{ISO}} H_n(S) \tag{31a}$$

for rodlike chains. For the treatment leading to Eq. 29,

$$H_n(S) = \frac{3S(1 - S)^{7/2}(1 + S)^2(1 + 2S)^{1/2}}{(1 + S/2)} \tag{31b}$$

where S may be computed with Eq. 20a. Except for S near the critical value for mesophase formation, $\eta_n > \eta_0$ according to these results. Data on η_κ and $\nu^{(1)}/|\kappa|$ for a solution of PBG[20] given in Figure 5 show η_κ and $\nu^{(1)}/|\kappa|$ that tend together with decreasing κ. Definitive evidence on the constancy of η_0/η_n in slow flow is lacking, but it does appear that $\nu^{(1)}$ decreases with increasing S,[6] in qualitative accord with Eq. 31.

The expression for η_0 and η_n given above requires slow flow under the condition $\alpha_2\alpha_3 > 0$. Application of Eq. 1 to elongational flow gives a viscosity η_E in slow flow for any α_i:[31]

$$\eta_E = \alpha_1 + (3/2)\alpha_4 + \alpha_5 + \alpha_6 \tag{32}$$

Making use of Eq. 19, for rodlike chains,

$$\eta_E = \eta_0^{ISO} H_E(S) \tag{33a}$$

Alternative expressions for $H_E(S)$ are available for the two sets of $A_i(S)$ given in Table II:

$$H_E(S) = 3(1 - S)^3(1 + S)^2(1 + 2S); \qquad \text{Ref. 30} \tag{33b}$$

$$H_E(S) = (1 - S)^3(1 + S)^2(9 + 24S + 32S^2)/3; \text{ Ref. 31} \tag{33c}$$

where S is given by Eq. 20a or 20b in Eqs. 33b or 33c, respectively. In neither case does $\eta_E = 3\eta_0$ as is the case for isotropic fluids;[18] η_E decreases with increasing S in both cases.

An approximate treatment has been given for unstable slow shear flow ($\alpha_2\alpha_3 < 0$), predicting periodic tumbling of n under such circumstance.[23] According to this theory $\boldsymbol{n}$ tends to be in the flow plane ($\theta = 0$), but to alternate between alignments $\pm\ \phi_0$ out of the shear plane as the director tumbles rapidly ($\theta \neq 0$) between positive and negative ϕ_0, with a tumbling frequency ω_T given by

$$2\kappa/\omega_T = \{(|\alpha_2|/\alpha_3)^{1/2} + (\alpha_3/|\alpha_2|)^{1/2}\} \tag{35}$$

With the results in Table II for the theory with $\alpha_2\alpha_3 < 0$,[30] $|\alpha_2|/\alpha_3 = (4S - 1)/(1 - S)$, and $|\alpha_2|/\alpha_3 >> \alpha_3/|\alpha_2|$ unless S is very close to its critical value (i.e., $c \approx c_{NI}$). Consequently, $\omega_T \approx 2\kappa[(1 - S)/(4S - 1)]^{1/2}$.

The recoverable compliance R_κ determined after flow steady-state flow at shear rate κ is shown in Figure 4 for a nematic solution of PBT.[7] Values of $R(t)$ shown in Figure 6 for isotropic and nematic

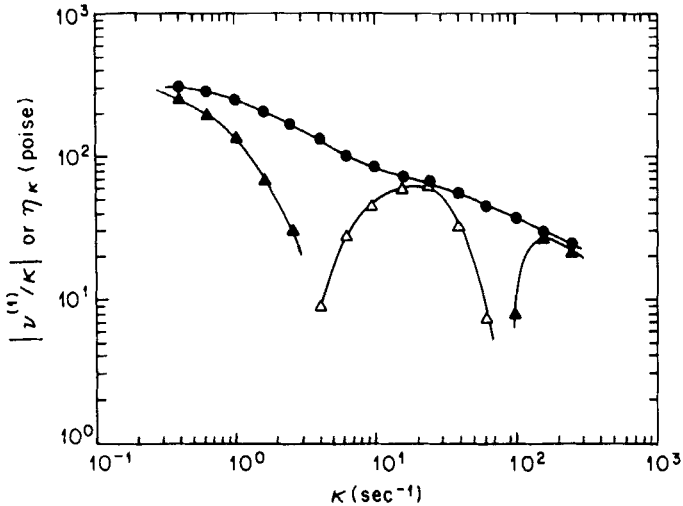

FIGURE 5 The shear viscosity η_κ (circles) and the absolute value $|\nu^{(1)}/\kappa|$ of the normal viscosity η_n (triangles) as functions of the shear rate κ for a liquid crystalline solution of PBG; $\nu^{(1)}$ is positive for filled triangles and negative for unfilled triangles. (After Reference 52).

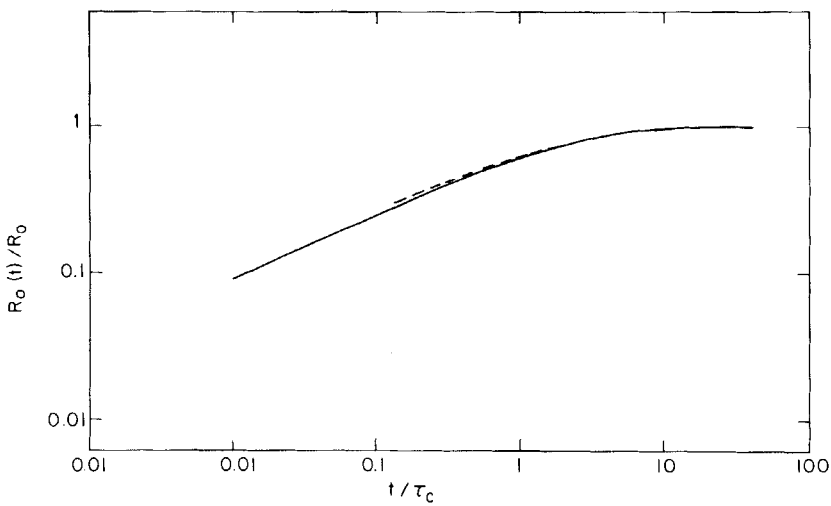

FIGURE 6 The recoverable compliance $R_0(t)$ divided by its limiting value $R_0 = R_0(\infty)$ versus the reduced time t/τ_C, for solutions of PBT, where $\tau_C = \eta_0 R_0$ for a nematic solution; dashed and solid curves are for isotropic and nematic solutions, respectively. (After Reference 7).

solutions of PBT were determined from the recovery on cessation of steady flow, with $\eta_0 R_0 \kappa < 1$ or $\eta_p R_0 \kappa < 1$ for isotropic and nematic solutions, respectively.[7] As seen in Figure 6, the reduced plots of $R(t)/R_0$ versus $t/\eta_p R_0$ or $t/\eta_0 R_0$ are similar. The origin of the viscoelastic effects observed with the nematic solution is presently unknown. It may involve flow induced nonuniformity in the director field discussed below in the paragraphs on flow birefringence.

Flow birefringence studies in slow steady-state flow (viscosity equal to η_p) suggest that the director field may not be as uniform as that predicted in connection with Eq. (26). Flow birefringence experiments have been attempted with a nematic solution of PBT prepared by extrusion between parallel glass disks—the solution was injected through a port in the center of the upper disk, and extruded radially between the parallel plates.[35] After being annealed for 10 hr., the sample exhibited low scattering and T_+ dependent on ψ as expected for preferential alignment in the radial direction, with a field of disclinations near either bounding surface. Flow was performed by rotation of the lower disk at angular velocity Ω, with the upper plate fixed. For the flow pattern expected with an isotropic fluid, the shear rate κ is given by $\Omega r/h$ in this geometry, where r is the distance from the center and h the plate separation (300 μm in the arrangement used). In this flow one solution to Eq. (1) allows stable flow with a viscosity given by $\eta_a = \alpha_4/2$ if $\Omega r/h$ is small enough.[10] The flow is unstable toward perturbations of $\boldsymbol{n}$, and various complicated flows predicted with increasing Ω[10,15,16] have been observed with small molecule nematogens.[15] In slow flow of a nematic PBT solution with initial preferential alignment in the radial direction at rest, optical effects indicating complex effects on the director field were observed for the lowest Ω used in steady shear ($\Omega r/h \approx 10^{-2} s^{-1}$) and in slow oscillatory motion, with frequency $10^{-3}\, s^{-1}$.[35] Shortly after the onset of steady shear (strain less than 2), defects with the appearance of disclinations appeared—similar effects have been reported with other polymeric nematogens.[39] With increased strain, turbid regions developed throughout the fluid, merging to encompass the entire sample. Under these conditions, $T_+ \approx T_\parallel$, with $T_+ + T_\parallel < 1$, presumably due to attentuation by scattering, i.e., $K_\gamma < 1$, see Eq. (11). Similar behavior is observed in flow of nematic solutions of PBT through a rectangular channel[35] and with other nematic solutions in torsional flow.[3,40] In such cases, the birefringence cannot be determined owing to the strong scattering. Similar behavior is observed in slow flow for a sample with a mottled texture at rest.[7,35]

The fluid appears grainy under conditions of slow flow with sup-

pressed $T_+ + T_\parallel$,[34,40–46] motivating consideration of a flow in which (deformable) domains, each with a nearly uniform $\boldsymbol{n}$ tumble past each other, perhaps with $\boldsymbol{n}$ more-or-less random among the domains.[3,4] This flow has been modeled for a fluid with $\alpha_2\alpha_3 < 0$ (see below), assuming a dense field of disclinations corresponding to the boundaries between "domains."[23,42] It seems unlikely that true disclinations exist in either the mottled texture at rest, or the fluid in flow starting from such a texture—both are too far from equilibrium in polymeric fluids. Unstable flow may produce textural features that propagate to produce a microstructure with relatively large spatial gradients in $\boldsymbol{n}$. The formation of more-or-less well defined domains, each comprising a nematic with a particular $\boldsymbol{n}$, but all with the same S seems unlikely—the gradient in $\boldsymbol{n}$ would be very large at the domain boundaries. The latter could exist, however, if the boundary between domains comprised poorly ordered material, perhaps even isotropic, in which case the high viscosity in the disordered phase could stabilize the domain structure at rest or in a very slow flow. Another alternative is that discrete domains do not exist, but rather that $\boldsymbol{n}$ is continuous, with quasi-periodic tumbling of $\boldsymbol{n}$ along the flow direction, coupled with substantial, quasi-periodic fluctuations of $\boldsymbol{n}$ out of the shear plane, resulting in strong scattering and a grainy appearance.

As mentioned above, if $\alpha_2\alpha_3 < 0$, shear flow is predicted to cause $\boldsymbol{n}$ to tumble between orientation $\pm\,\phi_0$ out of the shear plane in the plane of flow ($\theta = 0$). It has been suggested that the spatial extent over which such tumbling is coherent will be of order $(K/\sigma)^{1/2}$, where K is a "characteristic" Frank elastic constant and σ is the shear stress.[23] For small σ coherence of ϕ_0 among these regions is not expected, with the result that the scattering would be strong and the flow birefringence weak.

On cessation of slow steady flow, $T_+ + T_\parallel$ increases gradually for nematic solutions of PBT, with $T_+(\psi = \pi/4)$ exhibiting successive minima and maxima with increasing time.[35] Similar results obtained for nematic solutions of PBG are shown in Figure 7[43] (these data were obtained following steady flow with $\eta_p R_0 \kappa \approx 1$). The relaxation toward a smooth texture ($T_+ + T_\parallel$ near unity) proceeds over a time long compared with the relaxation time $\eta_p R_0$, e.g., $t/\eta_p R_0$ is about 10^4 for the largest t in Figure 6. This is much larger than the value of $t/\eta_p R_0$ for which the viscoelastic recovery is essentially complete (see Figure 5). The small $T_+(\psi = 0)$ and large $T_+(\psi = \pi/4)$ at longer relaxation time is consistent with alignment of $\boldsymbol{n}$ along the former flow direction. This may indicate a preferred alignment of $\boldsymbol{n}$ in the flow direction in slow flow even though substantial deviations dis-

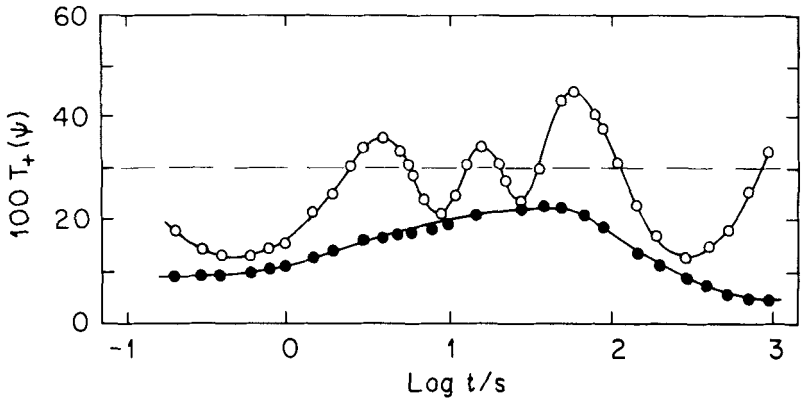

FIGURE 7 The transmission of $T_+(\psi)$ between cross polars for a nematic solution of PBG as a function of the time t after cessation of steady flow; ψ is $\pi/4$ or 0 for open circles and filled circles, respectively. The dashed line shows the level of $T_+(\pi/4)$ in steady flow. (After Reference 43).

cussed above lead to a strong scattering. In this case, η_p may be about equal to η_0 expressed by Eq. 26. It remains to be seen whether the fluctuations in $\boldsymbol{n}$ are better considered as discrete domains or as more continuous, and to definitively identify their source(s).

Behavior in anomalous slow flow

Although the anomalous flow behavior at small κ is reminiscent of effects observed in certain forms of yield (i.e., transition from solid to fluid viscoelastic behavior),[47] detailed studies on nematic solutions of PBT and PPTA show them to be fluidlike under as low a shear stress as could be used.[7] Moreover, in anamolous flow $-\partial \ln \eta_\kappa / \partial \ln \kappa$ is not as large as unity, as would be the case if yield from solid to fluid behavior occurred. An alternate explanation for anomalous behavior in very slow flows considers the effects of nonzero h owing to the effects of adsorbed layers at the planes bounding the sample, and their effect on the alignment angle θ.[16] The magnitude of these effects depends on the dimensionless Ericksen numbers E_i[10,14,16] given by

$$E_i = (\eta_i/K_i)Vd = (\eta_i/K_i)d^2\kappa \tag{36}$$

where i may indicate splay, twist or bend, depending on the nature of the surface alignment, and V is the relative velocity of surfaces separated by distance d. It is convenient to express E_i in the form $E_i = k(\eta_i/K_i)(\eta_p R_0 \kappa)$ where $k = d^2/\eta_p R_0$ depends on the apparatus (d) and the sample ($\eta_p R_0$). Anomalous flow often develops for $\eta_p R_0 \kappa$

< 0.1. If the appropriate E_i is large, then $\theta \approx \theta_0$ everywhere except perhaps very near the surfaces, and the viscosity calculated as the stress divided by the nominal strain rate is equal to η_0 (provided $\eta_0 R_0 \kappa < 1$). If the appropriate E_i is small, then θ is controlled by the alignment at the surface, and the viscosity is not given by η_0. For example, if the orientations θ_1 and θ_2 at the surfaces are in the plane of the surfaces and along the flow directions, then the viscosity is given by η_b for very small E_i. An approximate theory[16] based on Eqs. 1 and 2 for $\boldsymbol{n}$ everywhere in the plane of shear gives the nominal viscosity

$$\eta_\delta = \eta_0\{1 - E^{-1/2}C(\theta_1,\theta_2,\theta_0,E)\}^{-1} \tag{37}$$

as a function of E for fluids with $\alpha_2\alpha_3 > 0$; C is positive if θ_1 and θ_2 exceed θ_0. For the PBT solution identified in Table I, anomalous flow occurs with $\eta_p E_0 \kappa < 0.1$ using an apparatus such that $k = 10^{-8}$s/cm^2. With the data in Table I, $\eta_B/K_B > 4$ Pa·spN^{-1} so that $E_S^{1/2} \approx 15$ for $\eta_p R_0 \kappa = 0.1$, showing that η_δ could exceed η_0 for $\eta_p R_0 \kappa < 0.1$ for this material.

Negative normal stress has been predicted on the basis of the Leslie-Ericksen constitutive equation for fluids with $\alpha_2\alpha_3 > 0$ (in slow flow), as a consequence of an adsorbed layer at the bounding surfaces, with orientation angles of the rods at the surface different from the orientation angle θ_0 in stable flow.[16] The behavior of $\nu^{(1)}$ is closely linked to that for η_δ discussed above, and the sign of $\nu^{(1)}$ is controlled by the orientation angle at the boundary and the Erickson number E_i, with negative values predicted at small E_i for conditions with η_δ much different than η_0. This does not correspond to the region of fast flow for which negative $\nu^{(1)}$ are reported, e.g., see Figure 5. Neither does the theory predict oscillation of the sign of $\nu^{(1)}$ with increasing E_i, nor would the predicted director alignment produce the banded optical effect noted below. Experimental situations appropriate to the theory have probably not been studied for nematic polymer solutions.

It has been suggested[48] that the large viscosity of polymeric fluids will make E_i very large for most V of interest, since the Frank elastic constants are not increased proportionately. The limiting form of Eq. (1) for infinite E_i, which corresponds to a theory for anisotropic fluids due to Ericksen,[49] has been used in numerical calculations of flow in complex two dimensional geometries.[48]

Behavior in fast flow

As defined alone, steady fast flow refers to shear rates such that $\eta_p R_0 \kappa > 1$, and η_κ decreases below η_p with increasing κ. For the data

shown in Figure 4, R_κ also decreased with increasing κ. The dependence of η_κ and R_κ may be represented by Eq. 3 using values of η_i and τ_i deduced from $R(t)$ determined on cessation of steady slow flow.[7] One effect of the dependence of η_κ on κ is to reduce the maximum in η_κ at a given κ, as a function of c at fixed L.[7,44,45] A nonlinear theory based on adaptation of Eq. (1) has been given for materials with $\alpha_2\alpha_3 > 0$.[50] In this generalization of the Leslie-Ericksen theory, η_κ involves an order parameter S_κ dependent on κ instead of the equilibrium order parameter S appearing in slow flow, e.g., see Eq. 27. As shown in Figure 7 curves of η_κ/η_0 versus $D_R\kappa$ are parametric in S, where the effective rotational diffusion constant D_R of the rodlike chains in the equilibrium nematic phase is given by

$$6D_R = \left[\frac{cRT}{M\eta_0}\right]\frac{(1 - S)^2(1 + 2S)(1 + 3S/2)}{(1 + S/2)^2} \tag{38}$$

for the model that gives Eq. (29) for $H_{Sh}(S)$. As should be expected, reduction of η_κ in nonlinear flow is largest for systems with smallest S. Thus, the flow curves have different shapes on a bilogarithmic plot, and cannot be superposed by multiplication of $D_R\kappa$ by a function of S. Similar behavior has been reported for nematic solutions of PBT.[7] The theoretical result qualitatively reproduces the observed suppression of the maximum in η_κ vs c at fixed κ.[9] It appears, however, that the uniform flow predicted by the treatment may not be observed in practice, see below.

Although Eq. (3) appears to have some use in representing the shear stress for nematic solutions, it does not reproduce an unusual negative first-normal stress difference first reported in studies on nematic solutions of PBG.[46,51] Results obtained for η_κ and $\nu^{(1)}$ for such a solution are shown in Figure 5.[52] Negative values of $\nu^{(1)}$ are observed with increasing κ, and $\nu^{(1)}$ is observed to oscillate between negative and positive values with increasing κ. In this range of κ, $T_+ + T_\parallel$ has increased toward values expected in the balance of scattering losses, but $T_+(\psi = \pi/4)$ exhibits oscillations as a function of time.[34,52] Flow with a negative normal stress for nematic solutions of PBG has been associated with the appearance of alternating dark and bright striations in the light transmitted between crossed polars with the polarizer oriented at 45 deg. to the flow direction.[52] This optical effect implies a strong spatial coherence in $\boldsymbol{n}$, with $\boldsymbol{n}$ executing more-or-less periodic excursions around the flow direction, producing spatial arrangements of $\boldsymbol{n}$ similar to those discussed above in the section on magnetic field effects. Such tumbling behavior could correspond to

the large fluctuations observed in T_+ with $\psi = 45$ deg. in flow of nematic solutions of PBT with $\eta_p R_0 \kappa > 1$.

Some of the effects observed optically have been obtained in calculations based on Eq. (1) for materials with $\alpha_2\alpha_3 < 0$ (unstable shear flow). In this treatment, which is an extension of the calculation leading to Eq. 35, it is suggested that the characteristic dimension $(K/\sigma)^{1/2}$ of the regions of coherent tumbling decreases with increasing flow rate, until it becomes small enough that neighboring regions tend to correlate their tumbling motions.[23] This would lead to reduced scattering and increased birefringence relative to the behavior in slow flow, even though the birefringence would not be as large as expected in fully aligned flow. Moreover, the essential alternation of $\boldsymbol{n}$ between $\pm \phi_0$ would produce alternating bright and dark stripes normal to the flow direction for light transmitted between crossed polars, and would lead to negative $\nu_\kappa^{(1)}$.[23] As mentioned above, such effects have been observed for solutions of PBG.[52] Similar effects could occur in fast flow for a material with $\alpha_2\alpha_3 > 0$ (as determined, say, by light scattering methods) owing to the orientating effects of flow, which may be expected to tilt $\boldsymbol{n}$ toward the flow direction, making the flow unstable to perturbations. Further, it is suggested that viscoelastic effects may influence the size of the regions with coherent tumbling if $\tau\kappa >> 1$, with τ some relaxation time (e.g., $\eta_p R_0$ or $6D_R$). Consequently, nonlinear flow, with $\eta_\kappa < \eta_0$ is expected if $\tau\kappa >> 1$.

On cessation of flow, alternating dark and bright stripes orthogonal to the flow direction often appear for the sample between cross polars[52–56]—such optical features are not apparent in slow flow. In some cases alternating dark and bright bands normal to the flow direction are observed in focal planes above and below the mid-plane of the sample using polarized light (no analyzer), with light polarized along the former flow direction,[55] similar to the optical effects discussed above for flow induced in a magnetic field. The appearance of these optical features soon after cessation of flow is consistent with a tumbling flow. With increased time, the stripes disappear, and T_+ and $T_+ + T_\parallel$ increase slowly, the latter indicating decreased scattering as flow induced inhomogeneities are removed. After several hours (ca 50 hr), the texture is smooth, with low scattering, with the dependence of T_+ on γ very similar to that obtained for an isotropic fluid in flow, e.g., T_+ maximum for $\gamma = \pi/4$ and minimum for $\gamma = 0$, where γ is taken as the angle ψ between the polarizer direction and the flow lines.[35] During relaxation, $T_+(\gamma = \pi/4)$ is observed to pass through several maxima and minima as a function of time, presumably as δ changes through orders of π—similar effects have been reported for nematic solutions of PBG, as shown in Figure 8.[3,43,44]

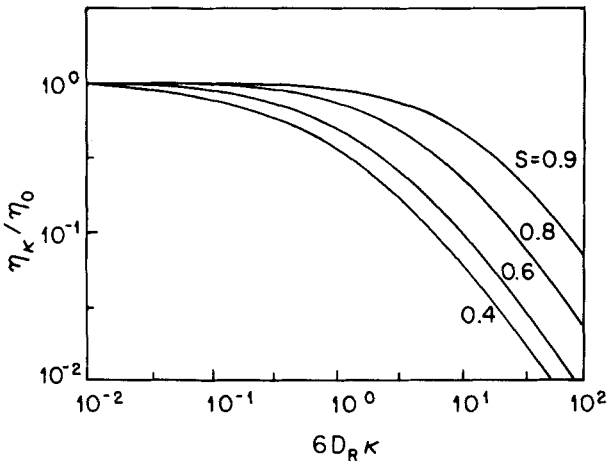

FIGURE 8 Theoretical prediction of η_κ/η_0 versus $6D_R\kappa$ as a function of the equilibrium order parameter S for nematic polymer solutions; D_R is the rotational diffusion constant. (After Reference 50).

Although $T_+(\gamma = 0)$ would be expected to be nil, as shown in Figure 8, it may be observed to increase during the relaxation showing that n is not exactly along the flow direction. Similarly, the extrema in $T_+(\gamma = \pi/4)$ are not as sharply defined as would be expected with good alignment of $\boldsymbol{n}$ along the flow lines. The $T_+(\gamma)$ exhibited after long relaxation indicates that the flow induced a preferential alignment of $\boldsymbol{n}$ with a component in the flow direction, even though the flow instability frustrated the attainment of this alignment during flow.

5. FUTURE DIRECTIONS

A number of features emerge from the preceding review. Experimental light scattering studies on monodomains of nematic solutions have barely begun. Systematic light scattering studies on rodlike chains as a function of c, L and T will go far toward establishing the usefulness of equilibrium theories expressing the Frank elastic constants and Leslie-Ericksen viscosity coefficients in terms of the equilibrium order parameter S. Moreover, the effects of chain flexibility intermolecular interactions side chain substituents, etc., have yet to be studied experimentally, although some theoretical predictions are available.[56,57] Similarly, the use of external fields (e.g., magnetic, electric, thermal, surface, etc.) to induce flow and reorient $\boldsymbol{n}$ has not been explored extensively or systematically with nematic solutions of

long chain polymers. Such studies provide a means to induce slow, controlled deformation, and as with work on small molecule nematogens, may provide valuable insight to the nature of flow induced inhomogeneities.

The effects of slow shearing flow on $\boldsymbol{n}$ remain ambigious. With the lack of much information on the Leslie-Ericksen viscosity coefficients, it is not certain whether slow shearing flow should be stable as a general rule. It may be that in the slow flow regime (viscosity independent of κ, equal to η_p) the flow is already fast enough to vitiate use of Eq. 1, and that the orientation angle θ is close enough to zero that the flow is effectively unstable toward perturbations. In that case, shear flow could result in tumbling of $\boldsymbol{n}$,[23] producing the optical behavior observed with several systems. Neither definitive experimental assessment of such effects nor theoretical analysis of flow stability are available. Similarly, viscoelastic behavior in the range of small κ remains to be explored systematically, either experimentally or theoretically. Such studies should be done on monodomain samples, for different director alignments. The role of surface alignment at very small κ discussed above requires as yet unperformed careful study—if important, such effects may complicate analysis of viscoelastic measurements.

The behavior in fast flow also requires additional study—shear rates in this range are often encountered in processing, making this region technologically as well as scientifically significant. A major unanswered question concerns the nature of the director field in fast shear flow. Conflicting evidence exists concerning its uniformity, but in most cases, it appears that $\boldsymbol{n}$ is not uniformly aligned in fast shearing flow. Systematic experiments (as a function of c, L, and T) are needed, along with a theoretical stability analysis and a general model to describe fast shear flow if $\boldsymbol{n}$ is not uniform. Such studies should include relaxation behavior on cessation of flow.

Acknowledgments

It is a pleasure to thank the National Science Foundation, Polymers Program, and the Air Force Office of Scientific Research for partial support in the preparation of this manuscript.

References

1. J. Hermans, Jr., *J. Colloid Sci.*, **17**, 638 (1962).
2. C.-P. Wong, H. Ohnuma and G. C. Berry, *J. Polym. Sci.: Polym. Symp.*, **65**, 173 (1978).

3. T. Asada, in *Polymer Liquid Crystals*, A. Ciferri, W. R. Krigbaum and R. B. Meyer, Eds., Academic Press, New York, 1982, Chapter 9.
4. K. F. Wissbrun, *J. Rheology*, **25**, 619 (1981).
5. S. P. Papkov, *Adv. Polym. Sci.*, **59**, 75 (1984).
6. D. G. Baird, in *Rheology*, Vol. 3, G. Astarita, G. Marrucci and L. Nicolais, Plenum Press, New York, 1980, p. 647.
7. Y. Einaga, G. C. Berry and S. G. Chu, *Polymer J.*, **17**, 239 (1985).
8. S. Venkatraman, G. C. Berry and Y. Einaga, *J. Polym. Sci., Polym. Phys.*, Ed., **23**, 1275 (1985).
9. M. Doi and S. F. Edwards, *The Theory of Polymer Dynamics*, Clarendon Press, Oxford, 1986.
10. F. M. Leslie, *Adv. Liq. Cryst.*, **4**, 1 (1979).
11. J. T. Jenkins, *Ann. Rev. Fluid Mech.*, **10**, 197 (1978).
12. P. G. deGennes, *The Physics of Liquid Crystals*, Clarendon Press, Oxford, 1974.
13. O. Parodi, *J. Phys.* (Paris), **31**, 581 (1970).
14. J. L. Ericksen, *Trans. Soc. Rheol.*, **13**, 9 (1969).
15. E. Dubois-Violette, G. Durad, E. Guyon, P. Mannerville and P. Pieranski, in *Liquid Crystals*, Ed. L. Liebert, *Suppl. 14, Solid State Physics*, Academic Press, New York, 1978, p. 147.
16. P. K. Currie, *J. Physique*, **40**, 501 (1979).
17. S.-G. Chu, S. Venkatraman, G. C. Berry and Y. Einaga, *Macromolecules*, **14**, 939 (1981).
18. G. C. Berry and D. J. Plazek, in *Glass: Science and Technology, Vol. 3 Viscosity and Relaxation*, D. R. Uhlmann and N. J. Kreidl, Academic Press, New York, 1986, Chapter 6.
19. D. G. Baird and R. L. Ballmann, *J. Rheol.*, **23**, 505 (1979).
20. T. Asada, T. Tanaka and S. Onogi, *J. Appl. Polym. Sci.: Appl. Polym. Symp.*, **41**, 229 (1985).
21. J. A. Odell, A. Keller and E. D. Atkins, *Macromolecules*, **21**, 289 (1983).
22. G. T. Keep and R. Pecora, *Macromolecules*, **18**, 1167 (1984).
23. G. Marrucci, *Pure and Appl. Chem.*, **57**, 1545 (1985).
24. R. W. Ditchburn, *Light*, 2nd. Ed., John Wiley, New York, 1963, p. 492.
25. K. Se and G. C. Berry, *Mol. Cryst. Liq. Cryst.*, in press.
26. V. Taratuta, A. J. Hurd and R. B. Meyer, *Phys. Rev. Lett.*, **55**, 246 (1985).
27. Groupe d'Etude des Crystaux Liquides d'Orsay, *J. Chem. Phys.*, **51**, 816 (1969).
28. J. P. van der Meulen and R. J. J. Zijlstra, *J. Physique*, **45**, 1627 (1984).
29. M. Miesowicz, *Nature* (London), **158**, 27 (1946).
30. G. Marrucci, *Mol. Cryst. Liq. Cryst. (Lett.)*, **72**, 153 (1982).
31. N. Kuzuu and M. Doi, *J. Phys. Soc. Jpn.*, **52**, 3489 (1983).
32. G. C. Berry, *Faraday Discuss. Chem. Soc.*, **79**, 141 (1985).
33. F. Lonberg, S. Fraden, A. J. Hurd and R. B. Meyer, *Phys. Rev. Lett.*, **52**, 1903 (1984).
34. Y. W. Hui, M. R. Kuzma, M. San Miguel and M. M. Labes, *J. Chem. Phys.*, **83**, 288 (1985).
35. M. Srinivasarao and G. C. Berry, to be published.
36. S. Chandrasekhar and U. D. Kini, in *Polymer Liquid Crystals*, A. Ciferri, W. R. Krigbaum and R. B. Meyer, Eds., Academic Press, New York, 1982 (Chapter 8).
37. N. V. Tabiryan, A. V. Sukhov and B. Ya. Zel'dovich, *Mol. Cryst. Liq. Cryst.*, **136**, 1 (1986).
38. B. D. Coleman and H. Markovitz, *J. Appl. Phys.*, **35**, 1 (1964).
39. N. J. Alderman and M. R. Mackley, *Faraday Discuss. Chem. Soc.*, **79**, 149 (1985).
40. H. L. Doppert and S. J. Picken, *Mol. Cryst. Liq. Cryst.*, in press.
41. M. Horio, S. Ishikawa and K. Oda, *J. Appl. Polym. Sci.: Appl. Polym. Symp.*, **41**, 269 (1985).
42. K. F. Wissbrun, *Faraday Discuss. Chem. Soc.*, **79**, 161 (1985).
43. T. Asada, Preprints, US-Japan Seminar on Polymer Liquid Crystals, June 14–20, 1983, Kyoto, Japan.

44. T. Asada, H. Muramatsu, R. Watanabe and S. Onogi, *Macromolecules*, **13**, 867 (1980).
45. G. Kiss and R. S. Porter, *J. Polym. Sci.: Polym. Phys. Ed.*, **18**, 361 (1980).
46. G. Kiss and R. S. Porter, *J. Polym. Sci.: Polym. Symp.*, **65**, 193 (1978).
47. E. C. Bingham, *Fluidity and Plasticity*, McGraw-Hill, New York (1922).
48. W. B. Van der Heyden and G. Ryskin, *J. Non-Newtonian Fluid Mech.*, **23**, 383 (1987).
49. J. L. Ericksen, *Arch Ration Mech. Anal.*, **4**, 231 (1960).
50. M. Doi, in *Theory and Applications of Liquid Crystals*, J. L. Ericksen and D. Kinderlehrer, Eds., Springer-Verlag, New York.
51. P. Moldenaers and J. Meuis, *J. Rheol.*, **30**, 567 (1986).
52. G. Kiss and R. S. Proter, *Mol. Cryst. Liq. Cryst.*, **60**, 267 (1980).
53. S. M. Aharoni, *Macromolecules*, **12**, 94 (1979).
54. P. Navard, *J. Polym. Sci.: Polym. Phys.* Ed., **24**, 435 (1986).
55. P. Navard and A. E. Zachariades, *J. Polym. Sci.: Polym. Phys. Ed.*, **25**, 1089 (1987), and references 1–18 cited therein.
56. R. B. Meyer, in *Polymer Liquid Crystals*, A. Cifeiri, W. R. Krigbaum, R. B. Meyer, Eds., Academic Press, New York, 1982, Chapter 6.
57. A. Stroobants, H. M. W. Lekkerkerker and T. Odijk, *Macromolecules*, **19**, 2232 (1986).